Chip Scale Optical Microresonator Sensors Integrated With Embedded Thin Film Photodetectors on Electrowetting Digital Microfluidics Platforms

Lin Luan, Matthew W. Royal, Randall Evans, Richard B. Fair, *Fellow, IEEE*, and Nan M. Jokerst, *Fellow, IEEE*

***Abstract*— Miniaturized, portable, sensitive, and low cost sensing systems are important for medical and environmental diagnostic and monitoring applications. Chip scale integrated photonic sensing systems that combine optical, electrical, and fluidic functions are especially attractive for sensing applications due to the high sensitivity of optical sensors, the small form-factor of chip scale systems, and the low-cost processing possible for systems fabricated with well-developed mass production techniques. In this paper, a chip scale sensing system, which is composed of a planar integrated optical microdisk resonator and a thin film InGaAs photodetector, is integrated with a digital microfluidic system. This system was designed, fabricated, and experimentally characterized by dispensing and moving droplets of glucose solution from the reservoir to the microresonator sensor. The optical output of the resonator was transduced by the integrated photodetector to an electrical current signal for readout.**

***Index Terms*— Chip-scale sensing systems, digital microfluidics, electrowetting, microresonator, photodetector, sensor.**

I. Introduction

LOW COST, rapid, miniaturized, portable sensing of chemical and biological analytes is critical to applications in the areas of medicine, environmental monitoring, and security. Chip scale integrated photonic sensing systems, which are inexpensive, small, low power, and sensitive, can be realized through the integration of thin film optical components with microresonators. The integration of such planar photonics sensing systems with digital microfluidics systems is attractive, because digital microfluidics systems can not only present liquid samples to the integrated optical sensing system, but can also carry out other complex functions, such as sample preparation, elsewhere on the chip using very low quantities of reagents [1]. This work explores the integration of an optical microresonator sensor with a photodetector to form a planar optical system that is integrated with a digital microfluidics system. The goal of this work is to move toward a fully integrated, chip-scale system for sample preparation and detection.

Optical microresonators, such as microdisk or microring resonators, are useful as fundamental building blocks in optical systems [2] as lasers, [3]–[5] filters, [6]–[8] and sensors [9]–[12]. For biological and chemical sensing, optical microresonator sensors are attractive because they can demonstrate high sensitivity and large dynamic range (in arrays) for quantitative sensing. Microresonators with high quality factor (Q) also have a low limit-of-detection [13]. High sensitivity microresonator sensors can be realized in a miniaturized, micron-scale device, and arrays of microresonator sensors can be fabricated to realize multiple analyte and high dynamic range sensing.

To create a portable optical sensing system, it is necessary to provide the sensor with an emitter, a detector, and waveguide interconnections. The most power efficient optical systems, important for low power portability, integrate these components directly with the sensor. Toward this end, planar polymer microring resonator sensors have been integrated with thin film photodetectors [14]. In this referenced work, polymer microring sensors were integrated with a thin film InGaAs-based metal-semiconductor-metal (MSM) photodetector on a Si substrate for chip scale sensing applications. The thin film photodetector was embedded in the optical waveguide output of the microresonator. The optical signal from the microresonator was detected by the photodetector, resulting in an electrical signal output. The output photocurrent from the photodetector varied as a function of wavelength and in proportion to the output optical power. Thus, the spectrum of the microring sensor could be measured by measuring the photocurrent at a series of wavelengths. As the spectral response of the microresonator shifted with index of refraction changes at resonator surface, the output current of the photodetector changed, thus showing the spectral shift with refractive index change. In the work reported herein, the thin film photodetector is embedded in the resonator output waveguide, and this optical system is integrated with an EWD microfluidic system.

Manuscript received September 27, 2011; accepted November 13, 2011. Date of publication December 9, 2011; date of current version April 25, 2012. This work was supported in part by Duke University, Durham, NC. The associate editor coordinating the review of this paper and approving it for publication was Prof. Gerald Gerlach.

L. Luan was with the Electrical and Computer Engineering Department, Duke University, Durham, NC 27708 USA. She is now with the Kuang-Chi Institute of Advanced Technology, Shenzhen, Guangdong 518000, China (e-mail: lin.luan@duke.edu).

M. W. Royal, R. Evans, R. B. Fair, and N. M. Jokerst are with the Electrical and Computer Engineering Department, Duke University, Durham, NC 27708 USA (e-mail: mwr9@duke.edu; rde@duke.edu; rfair@ee.duke.edu; nan.jokerst@duke.edu).

Color versions of one or more of the figures in this paper are available online at http://ieeexplore.ieee.org.

Digital Object Identifier 10.1109/JSEN.2011.2179027

Microfluidic lab-on-a-chip technology, which enables the miniaturization and integration of complex lab functions for sample preparation and detection, offers one possible solution for controlled, yet automatic, sample preparation. These systems are inexpensive, and also accurate, reliable, and well suited for medical applications in the developing world [15]. Electrowetting-on-dielectric (EWD) microfluidic systems enable electrical actuation of droplets of up to several microliters by modulating the interfacial tension between a liquid and an electrode coated with a dielectric layer. EWD microfluidic systems modify droplet wetting for polarizable and/or conductive liquids when they are in contact with hydrophobic, insulated electrodes. An electric field established between the dielectric layer and the ground results in an imbalance of the interfacial tension on the droplet surface if the electric field is applied to only one portion of the droplet, which forces the droplet to move [16].

For sensing applications, EWD microfluidic systems are advantageous in comparison to typical continuous fluidic systems. First, there are no moving parts, such as pumps or valves, since all the operations are carried out under direct voltage control. Thus, these systems are much smaller than typical continuous flow systems. Second, EWD enables multiple droplets to be controlled independently and simultaneously, since the electrowetting force is localized at the contact surface. This enables parallel processing of multiple droplets in the same system. Third, in sensing applications, it is possible to realize near 100% utilization of the sample or reagent, since no fluid is wasted for priming channels or filling reservoirs, in contrast to continuous flow microfluidics. Finally, EWD systems are extremely energy efficient: they generally consume nanowatts to microwatts of power per transfer, since there is very little electrical current passing through the electrodes [17].

The integration of optical sensing systems with EWD microfluidic systems is emerging. Few results have been reported to date. An integrated system based on the integration of an InGaAs-based thin-film photodetector sensor with a digital microfluidic system was first demonstrated in 2008 [16]. The first demonstration of a chip-scale optical microdisk/ring sensor integrated with a digital microfluidic system was published in 2009 [18]. Integrated optical/EWD systems are challenging to realize, since the optical system must be co-designed with the EWD system. This co-design must ensure that the optical system does not interfere with the electrowetting-based droplet transport, and vice versa, and that the EWD transport system delivers the correct volume and spatial orientation of the liquid analyte to the sensor for sensing. In addition, typical optical systems contain components such as photodetectors and emitters that are 500 microns thick. These components are difficult to integrate directly into the top plate of an EWD system, which is typically less than 150 μm thick.

To address these issues, this paper reports on the integration of thin film (one micron thick) photodetectors with thin film polymer microresonator sensors into an optical system, as shown in Figure 1(a). This optical system is integrated into the top plate of an EWD microfluidics system, so that the processed fluid from the EWD system addresses the sensor, as shown in Figure 1(b). The integrated system functionality was tested through the actuation and mixing of successive test glucose droplets by the EWD microfluidic system onto the microresonator sensor. The sensor responded to the index of refraction changes caused by the changes in glucose concentration at the sensor surface through shifts of the spectral output of the sensor. The optical output from the sensor was then transduced by the integrated photodetector to produce an electrical readout for the sensing system, as shown in Figure 1(b).

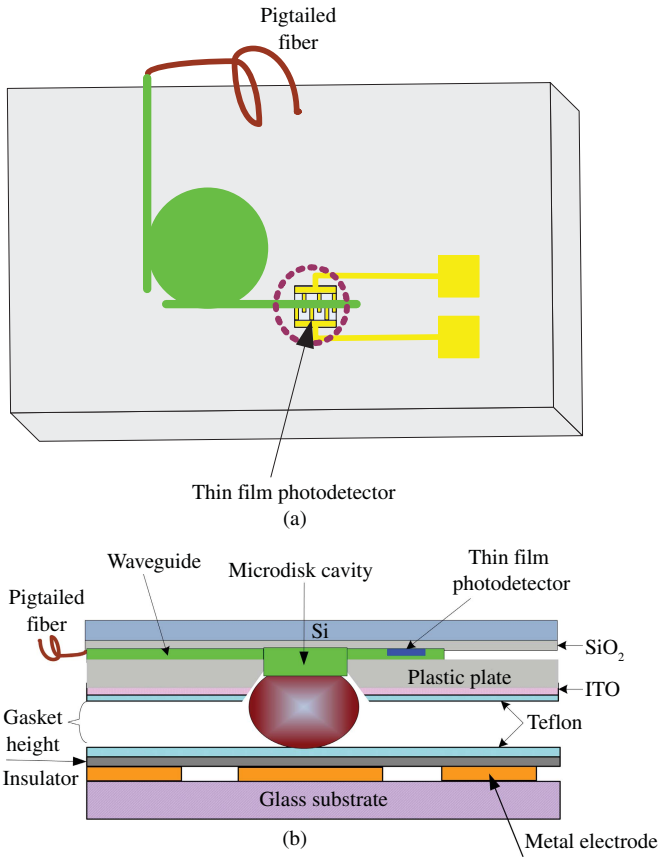

Fig. 1. (a) Top view of a microdisk resonator sensor integrated with a thin film InGaAs MSM photodetector. (b) Cross sectional view of the integrated optical system shown in (a) that has been integrated with an EWD digital microfluidic platform.

II. Fabrication and System Integration

The planar optical sensing system consisted of an optical microdisk resonator sensor integrated with a thin film InGaAs photodetector (PD) that was then integrated with an EWD digital microfluidic system, as shown in Figure 2. To fabricate the microresonator/PD optical sensing system, an InGaAs-based thin film MSM photodetector and an optical microresonator sensor were fabricated and integrated onto a SiO_2/Si substrate. First, the metal electrodes (Pt/Ti) to which the MSM would be bonded were deposited on the SiO_2/Si substrate. Next, a thin film MSM PD was fabricated separately and then inverted and bonded to the metal pads on the SiO_2/Si substrate. The material used to fabricate the MSM

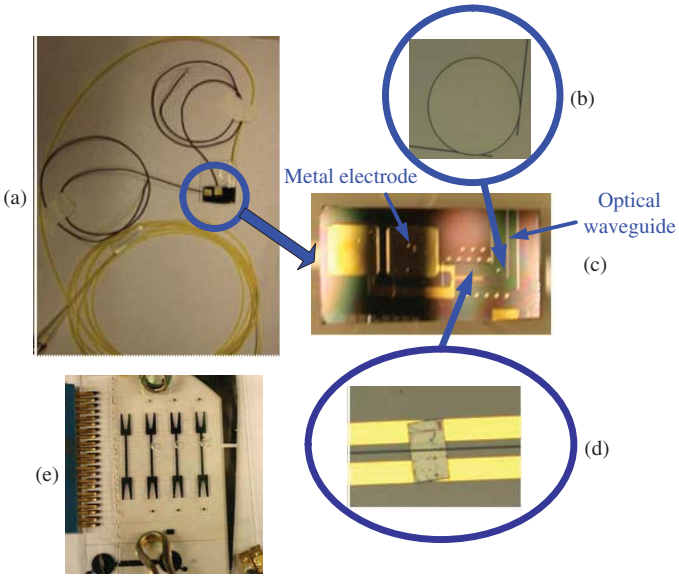

Fig. 2. Photographs of the integrated optical microresonator sensor/PD optical system integrated with an EWD microfluidics system. (a) Photograph of the optical microring resonator sensor integrated with an InGaAs photodetector on SiO_2/Si that has been bonded to a glass carrier. Single mode optical fibers are pigtailed to the optical waveguides. (b) Top view of the 600 μm diameter microresonator sensor on SiO_2/Si. (c) Photomicrograph of the integrated optical system on SiO_2/Si (microresonator sensor, waveguides, InGaAs thin film MSM photodetector). (d) Photomicrograph of the MSM thin film photodetector embedded in an optical output waveguide. (e) Photomicrograph of the digital microfluidic system to which the integrated optical system was bonded.

photodetectors was grown by molecular beam epitaxy on an InP substrate. The grown layers consisted of a 40 nm InAlAs (cap layer), 20 nm InGaAlAs (superlattice graded layer), 800 nm InGaAs (absorbing layer), 200 nm InAlAs (window cladding layer), and a 200 nm InGaAs (selective etch stop layer), with all of the layers nominally undoped. Metal fingers (Ti/30nm-Pt/40nm-Au/200nm) were defined on the MSM with photolithography and a lift off process. The next step was mesa etching with H_2O_2/citric acid. The etched MSM mesas were then coated with Apiezon W and immersed in HCl, which selectively removed the InP substrate. Next, the MSM devices were bonded to a transparent transfer diaphragm, and the Apiezon W was removed with TCE. Finally, the MSM devices were transferred (and, in that transfer, inverted) aided by a droplet of water and bonded to the metal pads on the SiO_2 (4 μm thick)/Si host substrate. The photodetector to pad metal/metal contact bond was then annealed by heating at 180 °C for 20 minutes to improve the mechanical strength. The fingers of the photodetector were 2 μm by 30 μm and the spacing between the fingers was 3 μm. The total MSM area was 110 μm by 245 μm with a 100 μm by 150 μm contact area and a 35 μm by 100 μm sensing area. Note that the MSM electrodes will lie on the opposite side from the waveguide. Next, the microresonator sensor was fabricated as described in [19]. The 5 μm wide SU-8 output and tapered input waveguides (~2.3 μm thick, with the taper 15 μm wide at the input port and 5 μm wide at the taper end) were patterned on top of the photodetector on the Si, as shown in Figure 1(b). Next, a 300 nm thick PMMA layer, intended to be the interlayer dielectric, was spin coated. To complete the optical system, a 2.35 μm thick SU8-2002 microresonator cavity that was 600 μm in diameter was patterned, as shown in Figure 2(b). To address the microresonator sensor and the MSM PD when the optical system was integrated with the digital microfluidic system, the input port of the optical waveguide was pigtailed with a single mode optical fiber using optical adhesive. To electrically connect the PD, the metal PD electrodes were connected to external copper wires. Figure 2(a) is a photograph of an optical microdisk sensor integrated onto a Si/SiO_2 subtrate that has been adhesively bonded to a glass carrier and fiber pigtailed.

The electrowetting microfluidic system includes both a top plate and a bottom plate and is shown in Fig. 2(e). To fabricate the bottom plate of the electrowetting microfluidic systems, Cr electrodes were deposited and patterned on a transparent glass substrate to monitor the movement of the droplets. An 80 μm thick SU-8-3050 gasket was next patterned on the bottom plate, followed by vacuum deposition of a high dielectric paralyene layer and a spin coated layer of hydrophobic Teflon. A layer of transparent, conductive indium tin oxide (ITO) was sputter desposited on the top acrylic plastic plate followed by a spin coated layer of Teflon. A tapered and hydrophilic via (1000 μm diameter) was drilled into the top plate so that the fluid in the EWD system could address the sensor located in the top plate via. The drilling process used caused the via acrylic to be roughened, thus producing a hydrophilic via surface.

The integrated optical sensing/PD structure was then inverted and bonded to the microfluidic system with adhesive areas, such that the microresonator was centered in the via in the top plate of the microfluidic system and the acrylic layer served as the upper cladding for the waveguides.

III. Experimental Measurements

The integrated optical system (microdisk resonator sensor, waveguides, and photodetector) was integrated with a digital microfluidic system. This microfluidic system was used to test the optical system by dispensing and actuating glucose droplets to the sensor. Merging glucose containing droplets with the solution in contact with the microresonator varied the index of refraction at the microresonator sensor surface in proportion to the glucose concentration.

As the glucose concentration presented to the optical microdisk resonator changed, the spectral output of the microresonator shifted. These spectral shifts were measured using a tunable laser and the photodetector integrated into the system. The input port of the pigtailed microdisk sensor was used to optically address the system. The optical signal from a HP 81618A tunable diode laser module (single mode output) was input to an erbium doped fiber amplifier (EDFA) to amplify the input laser signal. A half-wave plate was used to control the input laser polarization to the integrated sensor system to realize the optimum on-resonance transmitted power and extinction ratio. A single mode optical fiber that was pigtailed to the input optical waveguide was used to launch the polarized laser beam into the integrated optical system.

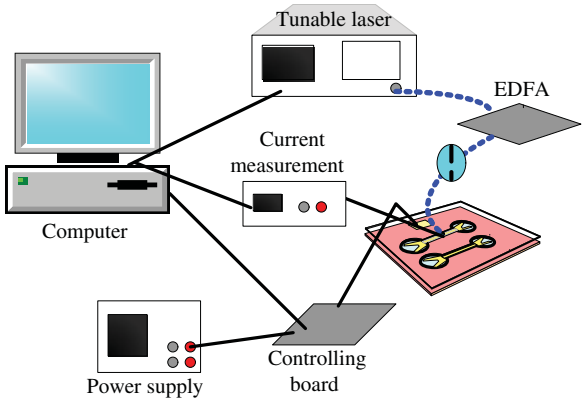

Fig. 3. Spectral measurement setup for the integrated optical/microfluidic system: a tunable diode laser and current/voltage measurement for the PD output. Blue dotted lines indicate optical connections, and black lines indicate electrical connections.

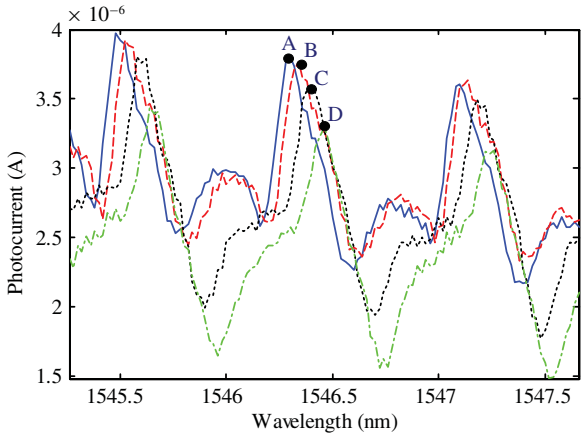

Fig. 4. Spectra of the microdisk resonator sensor (integrated with waveguides and a photodetector), read out as photodetector current, as a function of index of refraction (through varying glucose concentration at the resonator sensor surface). Solid line (A) is de-ionized water; long-dashed line (B) is 0.33 g/100 ml glucose solution; short-dashed line (C) is 1 g/100 ml glucose; long/short dashed line (D) is 1.8 g/100 ml glucose solution.

After the microdisk resonator sensor, the optical signal in the output waveguide was sensed by the thin film photodetector (embedded in the output optical waveguide), which was biased with a Keithley 236 Source Measurement Unit. Labview was used to control the tunable laser to sweep the input wavelengths from 1540–1560 nm in 20 pm increments, and the Keithley 236 Source Measurement Unit (SMU) was used to record the photodetector current output at 1–10 volt bias. When the input laser tuned to each wavelength, an output trigger signal was generated, which was received and taken as the input trigger by the Keithley SMU to measure the output photodetector current. After the current measurement was complete, the Keithley SMU would generate an output trigger, and this trigger would be sent to the tunable laser and taken as the input trigger of the laser to switch to next wavelength. In this manner, the laser tuned through the spectrum, as shown in Figure 3. Each spectral sweep took 240 seconds. A full spectral sweep was performed for each glucose concentration presented to the microresonator sensor by the microfluidics system.

To test the integrated microdisk sensor/PD/microfluidic system, test droplets were dispensed and actuated using voltage control (70 V peak-to-peak) of each electrode in the digital microfluidic system shown in Figure 2(e). A computer controlled relay board controlled the on/off switching of the electrodes, which in turn manipulated the droplets. Droplets were first dispensed from an on-board reservoir, then actuated from metal pad to metal pad using applied voltages, and thus were moved from the reservoir to the position where the via and microresonator sensor were located. When the droplets reached the via, the hydrophilic inner walls of the via caused the droplet to push up into the via to address the microresonator sensor at the top of the via.

A measurement of the spectrum of deionized water provided the baseline spectral data for the microresonator sensor. First, several droplets of water were dispensed from the on-board reservoir and presented to the sensor through the via to ensure the entire area of the resonator was covered with the solution during the sensing operation. Next, the reservoir was filled with glucose solution, which was actuated droplet by droplet to the sensor, where the droplets mixed with the previously dispensed water, thus generating increasing concentrations of glucose solution as droplets were added. The glucose concentrations, and thus, indices of refraction, were estimated using the volume of droplets dispensed and the known starting volume of deionized water presented to the microresonator through the via. These changes in glucose concentration resulted in a change in index of refraction at the microresonator sensor surface, which appeared as shifts in the resonant peaks in the output spectrum.

IV. Results and Data Analysis

As the index of refraction changed at the microresonator sensor surface (due to varying glucose concentrations), the output spectrum of the microresonator changed, thus changing the output optical signal into the output waveguide, which was sensed by the integrated photodetector. Representative spectral shifts are shown for multiple glucose concentrations in Figure 4. The baseline, water, is spectrum A. Subsequent dispensing and actuation of glucose droplets mixed with the water at the via, shown as spectrum B, C, and D, in order, show a consistent spectral shift with increasing glucose concentration.

After identifying the spectral peaks, the change in the peak position for different glucose concentrations (i.e. different indices of refraction) were calculated. The calculated resonant wavelength shifts are presented in Figure 5. These peak wavelength shifts were calculated by taking the difference in wavelength of the initial (deionized water) baseline and the resonant spectral peak position for each glucose concentration. Measurement uncertainties (represented by the error bars in Figure 5) include intensity noise, wavelength measurement noise, inaccuracy due to the limited wavelength resolution, resonant wavelength drift, and inaccuracy of the glucose concentration (the uncertainty in the total volume of the merged droplets accumulated as more droplets were merged with the solution in contact with the sensor). The five measured

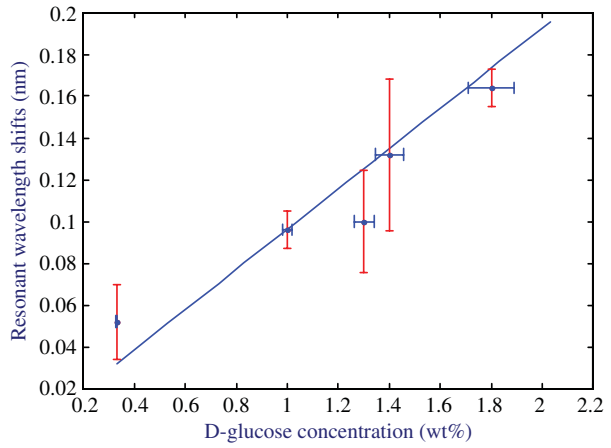

Fig. 5. Resonant wavelength shifts exhibited by the microdisk sensor for different concentrations of D-glucose in DI water.

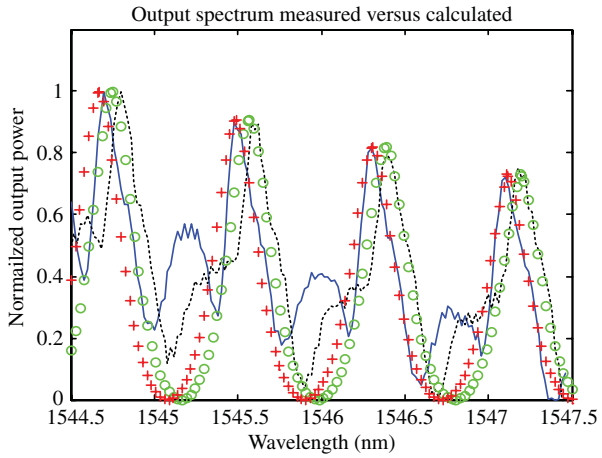

Fig. 6. Comparison of the measured and calculated normalized output spectral shifts of the integrated microdisk/waveguide/PD sensor with a 600 μm diameter. The solid and dotted lines show the measured spectrum shifts in the experiments from 0 wt% water (solid blue line) to 1 wt% (dotted black line) glucose solution, and the "+/o" denoted lines show the calculated spectrum shifts from 0 wt% water ("+" denoted line) to 1 wt% ("o" denoted line) glucose solution. The refractive index of the SU-8 used for this calculation was 1.57 [23].

resonant wavelengths (peaks from 1543.5-1547.5 nm, using the maximum point as the peak) used to calculate the data points were also used to calculate the error bars. The error bars are +/− one standard deviation for the peaks in the range of 1543.5–1547.5 nm. As is shown in Figure 5, the average resonant wavelength peak shifts rise approximately linearly with the increase in the glucose concentration. The index of refraction of the glucose solution is directly proportional to concentration of glucose in solution. The response of the fabricated microdisk sensor to the change in index of refraction at the resonator surface was measured to be 69 nm/RIU for this sensor, which is comparable to the sensitivity of the microdisk sensor measured in [20].

Sherry et al. [21] suggested a figure of merit (FOM) for comparing chemical sensor platforms that utilizes the full width half maximum (FWHM) of the resonance, which also influences the refractive index sensitivity of the system. This FOM is defined as the sensitivity (a linear regression of the index of refraction sensitivity) divided by the FWHM. Using this FOM, the integrated system studied herein has a FOM = (69 nm/RIU)/(0.35 nm, Peak "A")=197. It is important to compare sensors that can be integrated into a system and particularly planar sensors that can leverage current low cost planar micromanufacturing technologies, such as photolithography, since they do not require nanolithographic fabrication techniques. It is possible to achieve much higher FOMs by using nanolithographic definition of the bus waveguide and microresonator sensor [9, 22], but this would also substantially raise the cost of the integrated system.

A theoretical power throughput analysis was also conducted for the integrated microresonator/waveguide/PD structure. The laser output power from the single mode fiber was 4 mW. Coupling from the single mode fiber into the waveguide was very lossy with a coupling efficiency typically ranging from 0.1%-5%. Assuming symmetric coupling, the coupling efficiency from both the input waveguide to the microdisk and from the microdisk to the output drop waveguide is about 83.5%. The coupling efficiencies were estimated using a curve fit of the theoretical transmission spectrum, which contains the coupling coefficients as parameters as described in [10], to the measured transmission spectrum. Figure 6 shows the normalized measured microdisk resonantor/PD photocurrent (water base line shown in Figure 4 as the solid line) versus wavelength, as well as the simulated transmission profile ('+' and 'o' lines) calculated using the coupling efficiencies above. Figure 6 also shows the measured spectral shift from the water baseline to the spectra for 1 weight percent of glucose, shown as the dashed line, again using the coupling efficiencies above. The side lobes in the measured output spectra arise from higher order whispering gallery modes.

To predict the photocurrent from the integrated microresonator/waveguide/PD system, the coupling efficiencies, system losses, and the photodetector responsivity were used. The surface normal responsivity of the photodetector was measured at $\lambda = 1.55$ μm and was 0.39 A/W. Two-dimensional finite difference time domain (FDTD) simulation (Rsoft) was used to calculate the coupling efficiency of the optical power from the waveguide coupled into the photodetector. The calculated power absorbed by the PD radiated from the waveguide was 85% of the incident power in the waveguide. Using these losses and the photodetector responsivity, the range of output currents expected to be measured with the photodetector at a resonance peak was estimated to be between 0.77 μA and 38.6 μA. The resonance peaks observed in the measured photocurrent (Figure 4) have transmitted power of about 3.8 μA, which lies within the predicted range.

V. Conclusion

The co-design, fabrication, and test of a chip scale microdisk/PD optical sensing system integrated with an EWD digital microfluidic system was described in this paper. A microdisk resonator and waveguides were integrated with a thin film InGaAs MSM photodetector onto a SiO_2/Si substrate with the photodetector embedded in the output polymer optical waveguide of the microdisk resonator. After integration of

this optical system with an EWD microfluidics system, this integrated sample preparation and sensing system was able to detect changes in index of refraction as presented by glucose solutions in small droplets with different concentrations that were delivered by the microfluidics system. The measured wavelength shift and the corresponding resonant mode profiles were calculated and fit the experimental data well. A power throughput analysis was completed and the measured photocurrent from the optical system was within the range of the expected values, given the estimated system losses, coupling efficiencies, and photodetector responsivity. This integrated system is a significant step toward a more sophisticated optical system integration with a microfluidics platform that would support medical diagnostics and environmental monitoring.

REFERENCES

[1] N. M. Jokerst, S.-Y. Cho, L. Luan, M. Royal, and S. Palit, "Chip scale integrated microresonators for sensing applications," *Proc. SPIE*, vol. 6872, pp. 68720Q-1–68720Q-14, Feb. 2008.

[2] V. S. Ilchenko and A. B. Matsko, "Optical resonators with whispering-gallery modes-part II: Applications," *IEEE J. Sel. Topics Quantum Electron.*, vol. 12, no. 1, pp. 15–32, Jan.–Feb. 2006.

[3] A. Kapsalis, D. Syvridis, M. Hamacher, and H. Heidrich, "Broadly tunable laser using double-rings vertically coupled to a passive waveguide," *IEEE J. Quantum Electron.*, vol. 46, no. 3, pp. 306–312, Mar. 2010.

[4] S. L. McCall, A. F. J. Levi, R. E. Slusher, S. J. Pearton, and R. A. Logan, "Whispering-gallery mode microdisk lasers," *Appl. Phys. Lett.*, vol. 60, pp. 289–291, Jan. 1992.

[5] J. Van Campenhout, P. Rojo-Romeo, P. Regreny, C. Seassal, D. Van Thourhout, S. Verstuyft, L. Di Cioccio, J. M. Fedeli, C. Lagahe, and R. Baets, "Electrically pumped InP-based microdisk lasers integrated with a nanophotonic silicon-on-insulator waveguide circuit," *Opt. Exp.*, vol. 15, no. 11, pp. 6744–6749, 2007.

[6] Z. Shengmei, C. Hui, and A. W. Poon, "Microring-resonator cross-connect filters in silicon nitride: Rib waveguide dimensions dependence," *IEEE J. Sel. Topics Quantum Electron.*, vol. 12, no. 6, pp. 1380–1387, Nov.–Dec. 2006.

[7] R. Grover, T. A. Ibrahim, S. Kanakaraju, L. Lucas, L. C. Calhoun, and P. T. Ho, "A tunable GaInAsP-InP optical microring notch filter," *IEEE Photon. Technol. Lett.*, vol. 16, no. 2, pp. 467–469, Feb. 2004.

[8] J. V. Hryniewicz, P. P. Absil, B. E. Little, R. A. Wilson, and P. T. Ho, "Higher order filter response in coupled microring resonators," *IEEE Photon. Technol. Lett.*, vol. 12, no. 3, pp. 320–322, Mar. 2000.

[9] C. Y. Chao, W. Fung, and L. J. Guo, "Polymer microring resonators for biochemical sensing applications," *IEEE J. Sel. Top. Quantum Electron.*, vol. 12, no. 1, pp. 134–142, Jan.–Feb. 2006.

[10] S.-Y. Cho and N. M. Jokerst, "A polymer microdisk photonic sensor integrated onto silicon," *IEEE Photon. Technol. Lett.*, vol. 18, no. 20, pp. 2096–2098, Oct. 2006.

[11] A. Yalcin, K. C. Popat, J. C. Aldridge, T. A. Desai, J. Hryniewicz, N. Chbouki, B. E. Little, O. King, V. Van, S. Chu, D. Gill, M. Anthes-Washburn, and M. S. Unlu, "Optical sensing of biomolecules using microring resonators," *IEEE J. Sel. Top. Quantum Electron.*, vol. 12, no. 1, pp. 148–155, Jan.–Feb. 2006.

[12] S. Yuze, S. I. Shopova, G. Frye-Mason, and F. Xudong, "Rapid chemical-vapor sensing using optofluidic ring resonators," *Opt. Lett.*, vol. 33, no. 8, pp. 788–790, 2008.

[13] K. J. Vahala, "Optical microcavities," *Nature*, vol. 424, pp. 839–846, Aug. 2003.

[14] S.-Y. Cho and N. M. Jokerst, "Integrated thin film photodetectors with vertically coupled microring resonators for chip scale spectral analysis," *Appl. Phys. Lett.*, vol. 90, no. 10, pp. 101105-1–101105-3, 2007.

[15] P. Yager, T. Edwards, E. Fu, K. Helton, K. Nelson, M. R. Tam, and B. H. Weigl, "Microfluidic diagnostic technologies for global public health," *Nature*, vol. 442, no. 7101, pp. 412–418, 2006.

[16] L. Lin, R. D. Evans, N. M. Jokerst, and R. B. Fair, "Integrated optical sensor in a digital microfluidic platform," *IEEE Sens. J.*, vol. 8, no. 5, pp. 628–635, May 2008.

[17] R. B. Fair, "Digital microfluidics: Is a true lab-on-a-chip possible?" *Microfluid. Nanofluid.*, vol. 3, no. 3, pp. 245–281, 2007.

[18] L. Luan, R. D. Evans, D. Schwinn, R. B. Fair, and N. M. Jokerst, "Chip scale integration of optical microresonator sensors with digital microfludics systems," in *Proc. IEEE Lasers Electro-Opt. Soc. 21st Ann. Meet.*, Nov. 2008, pp. 259–260.

[19] L. Luan, S.-Y. Cho, and N. M. Jokerst, "Vertically coupled polymer microdisk resonators fabricated by photolithography technique," in *Proc. Electron. Compon. Technol. Conf.*, Reno, NV, 2007, pp. 2035–2040.

[20] S. Y. Cho and N. M. Jokerst, "A polymer microdisk photonic sensor integrated onto silicon," *IEEE Photon. Technol. Lett.*, vol. 18, no. 20, pp. 2096–2098, Oct. 2006.

[21] L. J. Sherry, S. H. Chang, G. C. Schatz, R. P. Van Duyne, B. J. Wiley, and Y. N. Xia, "Localized surface plasmon resonance spectroscopy of single silver nanocubes," *Nano Lett.*, vol. 5, pp. 2034–2038, Oct. 2005.

[22] G. D. Kim, G. S. Son, H. S. Lee, K. D. Kim, and S. S. Lee, "Integrated photonic glucose biosensor using a vertically coupled microring resonator in polymers," *Opt. Commun.*, vol. 281, no. 18, pp. 4644–4647, Sep. 2008.

[23] S. M. A. Borreman, A. A. M. Kok, M. B. J. Diemeer, and A. Driessen, "Fabrication of polymeric multimode waveguides and devices in SU-8 photoresist using selective polymerization," in *Proc. IEEE/LEOS Benelux Chapt. Symp.*, Amsterdam, Netherlands, 2002, pp. 83–86.

Lin Luan received the B.S. degree in electrical engineering from Shandong University, Shandong, China, the M.E. degree in communication and information systems from Peking University, Peking, China, and the Ph.D. degree in electrical engineering from Duke University, Durham, NC, in 2001, 2004, and 2010, respectively.

She is currently a Vice President with the Kuang-Chi Institute of Advanced Technology, Shenzhen, China. Her current research interests include photonic biochemical microresonator sensors integrated with digital microfluidic systems.

Matthew W. Royal received the B.S. degree in engineering science from Pennsylvania State University, State College, and the M.S. degree in electrical engineering from Duke University, Durham, NC, in 2006 and 2008, respectively. He is currently pursuing the Ph.D. degree in electrical engineering with Duke University.

He was supported by the National Defense Science and Engineering Graduate Fellowship for research and development of microresonator biosensors from 2007 to 2010.

Randall Evans photograph and biography not available at the time of publication.

Richard B. Fair (S'63–M'75–SM'75–F'90) received the Ph.D. degree from Duke University, Durham, NC, in 1969.

He spent 12 years with Bell Laboratories, Murray Hill, NJ, working on semiconductor devices and integrated-circuit technology. He spent 13 years as a Vice President with Microelectronics Center, Durham, having responsibilities in chip designs, computer-aided designs, packaging, process technology, and microelectromechanical systems (MEMS). He is currently a Professor of electrical and computer engineering with Duke University. He has published over 150 papers in refereed journals and conference proceedings, written ten book chapters, edited nine books or conference proceedings, and given over 120 invited talks, mostly in the area of semiconductor devices or the fabrication thereof. His research group first demonstrated microdroplet transport over electrode arrays based on electrowetting actuation. His current research interests include bio-MEMS and digital microfluidic chips.

Dr. Fair is a fellow of the Electrochemical Society and past Editor-in-Chief of the PROCEEDINGS OF THE IEEE. He has served as an Associate Editor of the IEEE TRANSACTIONS ON ELECTRON DEVICES. He is a recipient of the IEEE Third Millennium Medal in 2000 and the Solid State Science and Technology Prize and Medal from the Electrochemical Society in 2003, which was presented in Paris, France.

Nan M. Jokerst (F'03) received the Ph.D. degree in electrical engineering from the University of Southern California, Los Angeles, in 1989.

She is J. A. Jones Professor of electrical and computer engineering with Duke University, Durham, NC. She has published more than 250 papers in refereed journals and conference proceedings, three book chapters, and has four patents awarded in the areas of chip-scale integrated systems, sensors, integrated photonics, optical interconnections, and metamaterials.

Prof. Jokerst received the IEEE Education Society/Hewlett Packard Harriet B. Rigas Medal in 2002 and the IEEE Millennium Medal in 2000. She is a fellow of the Optical Society of America in 2000. She is a DuPont Young Faculty Awardee and the National Science Foundation Presidential Young Investigator, and has won a Newport Research Award, three teaching awards, and was a Hewlett Packard Fellow. She has organized and served on numerous conference committees, including the Board of Directors of the Optical Society of America as the Chair of the Engineering Council, the IEEE Lasers and Electro-Optic Society Board of Governors as an Elected Member, as the Vice President of Conferences, and as the Vice President of Technical Affairs. She has also served as the Elected Chair, Vice Chair, Secretary, and Treasurer of the Atlanta IEEE Section.